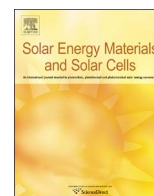




ELSEVIER

Contents lists available at ScienceDirect

# Solar Energy Materials & Solar Cells

journal homepage: [www.elsevier.com/locate/solmat](http://www.elsevier.com/locate/solmat)

## Laser-induced local phase transformation of CIGSe for monolithic serial interconnection: Analysis of the material properties



C. Schultz<sup>a,\*</sup>, M. Schuele<sup>a</sup>, K. Stelmaszczyk<sup>a,c</sup>, M. Weizman<sup>a</sup>, O. Gref<sup>b</sup>, F. Friedrich<sup>b</sup>,  
C. Wolf<sup>c</sup>, N. Papathanasiou<sup>c</sup>, C.A. Kaufmann<sup>c</sup>, B. Rau<sup>c</sup>, R. Schlatmann<sup>a,c</sup>, V. Quaschnig<sup>a</sup>,  
F. Fink<sup>a</sup>, B. Stegemann<sup>a</sup>

<sup>a</sup> PVcomB/HTW Berlin - University of Applied Sciences, Wilhelminenhofstr. 75a, D-12459 Berlin, Germany

<sup>b</sup> PVcomB/TU Berlin, Semiconductor Devices, Sekr. E4, Einsteinufer 19, D-10587 Berlin, Germany

<sup>c</sup> PVcomB/Helmholtz-Zentrum Berlin für Materialien und Energie GmbH, Schwarzschildstr. 3, D-12489 Berlin, Germany

### ARTICLE INFO

#### Article history:

Received 8 October 2015

Received in revised form

15 June 2016

Accepted 11 July 2016

#### Keywords:

CIGSe

Laser

Phase transformation

Interconnection

Nanosecond pulses

Heat affected zone

Raman

### ABSTRACT

The change of electrical conductivity in chalcopyrite (i.e.,  $\text{Cu}(\text{In}_x, \text{Ga}_{1-x})\text{Se}_2$  or CIGSe) solar cells induced by nanosecond laser pulses is investigated as a function of the elemental composition and its spatial distribution. The underlying laser induced phase transformation process, which results in a decomposition of the CIGSe semiconductor and a modification of its elemental composition, is utilized to form the monolithic series interconnection between front and back contact in CIGSe based thin film solar cells. The results show a dependence of the composition of the CIGSe layer and the resulting series resistance on the applied laser fluence. Lower series resistance is primarily related to an enhanced fraction of copper, gallium and zinc in the laser transformed zone resulting from selective vaporization of absorber elements. For intermediate laser fluences ( $\sim 0.36 \text{ J/cm}^2$ ) a patterning process is established that allows reliable and high-quality series interconnection. Both, lower and higher laser fluences result in high series resistances due to incomplete phase transformation or damages of the back contact, respectively.

© 2016 Elsevier B.V. All rights reserved.

### 1. Introduction

Thin film solar cell technology enables a simplified production and a reduced consumption of resources compared to the conventional silicon wafer based technology [1]. One of the essential steps to reduce the cost of production is the integrated monolithic serial interconnection. It involves the patterning of the functional solar cell layers with very fine lines by selective material removal. Typically, three patterning steps, denoted by P1, P2, and P3, alternating with layer deposition are necessary to perform monolithic serial interconnection. The first (P1) and the third (P3) scribe determine the width of the cells whereas the second step (P2) creates the back-to-front connection via opening of the absorber layer. The area between the outer edges of the P1 and P3 scribes should be as small as possible, since it is electrically inactive and does not contribute to the conversion efficiency (so called “dead area”).

$\text{Cu}(\text{In}_x, \text{Ga}_{1-x})\text{Se}_2$  (or CIGSe) has been established as the most efficient thin-film technology with a record efficiency of 22.3% on a  $0.25 \text{ cm}^2$  laboratory cell [2]. Increasing the module size to an

industrial level requires structuring the module into a number of cells to limit the photocurrent and to increase the voltage. Typically, in industrial production of CIGSe solar modules only the P1 is done by laser scribing, while for the P2 and P3 mechanical needle scribing is still widely used due to the lack of common and reliable laser processes. Main challenges are the tolerance to spatial inhomogeneities particularly in the absorber layer, the selectivity of the process and the high heat sensitivity of CIGSe [3–5]. However, as compared to mechanical scribing, laser scribing offers several advantages like well-defined precise scribing lines and higher scribing speed. Thus, complete laser scribing of CIGSe modules promises better process control, smaller dead areas and therefore higher conversion efficiencies [6].

A comprehensive study of thin film scribing for CIGSe solar cells with different types of lasers was reported by Compaan et al. [7]. Though long ns pulses ( $> 250 \text{ ns}$ ) were successfully applied for damage-free P1 and P2 scribing, excessive melt formation was observed from the CIGSe layer itself. As a main limiting factor of ns laser CIGSe processing the phase transformation of semiconducting CIGSe to a metallic state close to the ablation area due to thermal effects was identified [3]. As a result shunts are created in the solar cell and reduce its conversion efficiency. According to the results of theoretical modeling, processing without damage is possible with ultra-short-pulse lasers [5]. Recently, complete

\* Corresponding author.

E-mail address: [christof.schultz@htw-berlin.de](mailto:christof.schultz@htw-berlin.de) (C. Schultz).

structuring of CIGSe solar cells (i.e., P1, P2 and P3) by laser ablation has been successfully demonstrated by application of 10 ps laser pulses [8–11] and evaluated as being competitive to conventional needle scribing [8]. P2 laser scribing was also successfully demonstrated on flexible stainless steel substrates [12] and by patterning from the substrate side [13]. Further optimization of particularly P3 ps laser scribing was achieved by subsequent thermal annealing [14].

As alternative to P2 laser ablation by ps pulses, the thermal nature of ns laser pulses can be beneficially used to locally phase transform the CIGSe layer into a highly conductive compound that provides the electrical connection between the front and back contact as introduced by Westin et al. [15] and Ruckh et al. [16]. Accordingly, heating of the CIGSe layer during the exposure of ns laser pulses initiates a decomposition of the chalcopyrite compound and a rearrangement of its elemental constituents. Consequently, partial vaporization of the absorber elements occurs, leaving a Cu-rich, highly conductive material which can form the P2 interconnect [17]. Thus, alternative P2 patterning is achieved by drawing conductive lines rather than removing the material. This process can be performed through the already deposited TCO layer and, thus, further simplifies the patterning process [8,18]. Recently, the crucial influence of the applied laser fluence on the serial and shunt resistances of solar cells with such phase transformed P2 interconnection were revealed [18,19].

The objective of this work is to deliberately control the thermal impact of ns laser pulses for the preparation of the P2 interconnect by local phase transformation of CIGSe into a highly conductive phase via optimization of the incident cumulated laser fluence. Moreover, we aim to reveal the mechanisms responsible for the increase of the conductivity in the transformed scribing lines by a detailed analysis of the influence of the applied laser fluence on the morphological, chemical, electrical and structural properties of the phase transformed area. For these measurement standard thin film- and surface-analytical techniques, such as scanning electron microscopy (SEM), energy-dispersive X-ray spectroscopy (EDX), Raman spectroscopy and atomic-force microscopy (AFM) were applied. From these insights, the range of the heat affected zone will be estimated, based not only on visible modifications of the layer surface, but rather on material modifications within the CIGSe layer in the vicinity of the scribe. With these findings the competitiveness of this approach with respect to conventional P2 and P3 patterning by mechanical needle scribing will be demonstrated.

## 2. Experimental details

### 2.1. Laser patterning setup

For laser patterning of the solar cell layers a high speed motion system (Rofin Baasel Lasertech) was used. This system consists of high-precision linear motor drives for the translation stages which can be moved with velocities of up to 1.2 m/s. The patterning tool is equipped with a Time Bandwidth laser source (Duetto) emitting 1064 nm as well as the frequency doubled and tripled wavelengths (i.e., 532 nm and 355 nm) with pulse durations of about 10 ps. The maximum power of 15 W can be achieved for infrared radiation while the repetition rate can be varied from 50 kHz up to 8.2 MHz. Furthermore, a nanosecond laser (SL 3 SHG PV, Rofin Baasel Lasertech) is integrated operating at 532 nm with a maximum power of 2 W. This laser is a Q-switched, diode-pumped solid state laser (DPSS) with a pulse-to-pulse energy stability of < 1.5%. Both laser beams possess Gaussian spatial intensity distributions. The focused beam diameters ( $2\omega_0$ ) were  $\sim 40 \mu\text{m}$  (ps, 1064 nm, P1),  $\sim 55 \mu\text{m}$  (ps, 532 nm, P3), and  $\sim 70 \mu\text{m}$  (ns, 532 nm, P2) as

determined by the Liu method [20]. For comparison, mechanical patterning was performed with an industrially used tungsten carbide tip with a nominal tip width of  $40 \mu\text{m}$ .

The P1 patterning of the molybdenum (Mo) back contact layer was performed using ps laser pulses at 1064 nm, whereas the P3 patterning was done with ps laser pulses at 532 nm [8]. For the phase transformation process (P2) the ns laser was used. In the present study the laser pulse durations at the corresponding pulse energies were about 30 ns at a pulse repetition rate of 50 kHz.

### 2.2. Sample preparation

The samples were prepared according to the baseline process established at the Competence Center for Thin-Film and Nanotechnology for Photovoltaics Berlin (PVcomB) [21]. The CIGSe absorber layer is deposited using a so-called “sequential” or “2-step” approach. At the PVcomB this involves selenization of a metal (Cu–In–Ga) precursor at atmospheric pressure in an elemental Se containing  $\text{N}_2$  atmosphere and is carried out in an R&D in-line tool, provided by Smit Thermal Solutions. This process has the potential to substantially drive down the production costs for the CIGSe absorber layer and is currently under development at the PVcomB with a reproducible baseline efficiency of  $\sim 12\%$ , and a top efficiency of 15.5% for pure selenide absorbers [22]. The samples are composed of the following layer sequence: 3.1 mm soda lime glass (SLG) substrate, 150 nm  $\text{SiO}_x\text{N}_y$  barrier layer, 850 nm Mo back contact including a thin layer of MoNa,  $\sim 1.6 \mu\text{m}$  CIGSe absorber layer, 40 nm CdS buffer layer and transparent conductive oxide (TCO) front contact (i.e.,  $0.85 \mu\text{m}$  ZnO:Al plus  $\sim 150 \text{ nm}$  i-ZnO). A summary of the material properties, relevant for laser ablation and phase transformation, is given in Table 1.

After layer deposition, the  $30 \times 30 \text{ cm}^2$  samples were separated into nine  $10 \times 10 \text{ cm}^2$  sub-panels, each accommodating 49 single cells. The P2 scribes of the cells of each subpanel were patterned line-by-line with different laser pulse energies, ranging from  $3.5 \mu\text{J}$  to  $9 \mu\text{J}$  corresponding to laser fluences of  $0.28 \text{ J/cm}^2$ – $0.73 \text{ J/cm}^2$ . With respect to the impact on the CIGSe layer, these laser fluences cover a range of slight modification of the CIGSe surface up to the ablation of the whole layer stack. The pulse to pulse overlap was around 98% related to the spot diameter. For the sake of comparison all samples were patterned using the same experimental setup. The conductive zone was formed by local, laser-induced phase transformation of the absorber layer (P2) after deposition of the Al-doped zinc oxide layer. In Fig. 1 the main cell components and the contact design are schematically shown.

### 2.3. Characterization techniques

The series resistances as a function of the laser fluence were derived from a set of patterned cells as described in the previous section. I–V measurements were performed using a home-built

**Table 1**  
Summary of selected properties of typical CIGSe solar cell constituents relevant for this work.

Element	Melting temperature (K) [33]	Enthalpy of vaporization (kJ/mol) (300 K)	Diffusion coefficient ( $\text{cm}^2/\text{s}$ )
Zn	693	120 [33]	–
Al	933	290 [33]	–
Cu	1357	300 [33]	$10^{-9}$ .. $10^{-8}$ (380 K) [28]
In	429	230 [33]	$1.5 \times 10^{-11}$ (400 K) [27]
Ga	303	254 [34]	$4 \times 10^{-11}$ (725 K) [27]
Se	490	95 [34]	$2 \times 10^{-13}$ .. $10^{-12}$ (700 K) [35]
Mo	2887	590 [33]	–

Download English Version:

<https://daneshyari.com/en/article/6534636>

Download Persian Version:

<https://daneshyari.com/article/6534636>

[Daneshyari.com](https://daneshyari.com)